THE DESIGN AND ANALYSIS OF A MICROSTRIP LINE WHICH UTILIZES CAPACITIVE GAPS AND MAGNETIC RESPONSIVE PARTICLES TO VARY THE REACTANCE OF THE SURFACE IMPEDANCE

A Thesis
Submitted to the Graduate Faculty
of the
North Dakota State University
of Agriculture and Applied Science

By

Jerika Dawn Cleveland

In Partial Fulfillment of the Requirements
for the Degree of
MASTER OF SCIENCE

Major Department:
Electrical and Computer Engineering

April 2019

Fargo, North Dakota

North Dakota State University
Graduate School

Title

THE DESIGN AND ANALYSIS OF A MICROSTRIP LINE WHICH

UTILIZES CAPACITIVE GAPS AND MAGNETIC RESPONSIVE

PARTICLES TO VARY THE REACTANCE OF THE SURFACE

IMPEDANCE

By

Jerika Dawn Cleveland

The Supervisory Committee certifies that this ***disquisition*** complies with North Dakota

State University's regulations and meets the accepted standards for the degree of

MASTER OF SCIENCE

SUPERVISORY COMMITTEE:

Dr. Benjamin D. Braaten

Chair

Dr. Daniel L. Ewert

Dr. Jeffery Allen

Approved:

April 26, 2019	Dr. Benjamin D. Braaten
Date	Department Chair

ABSTRACT

This thesis presents the work of using magnetic responsive particles as a method to manipulate the surface impedance reactance of a microstrip line containing uniform capacitive gaps and cavities containing the particles. In order to determine the transmission line's surface impedances created by each gap and particle containing cavities, a sub-unit cell that centers the gap and cavities was used. Shown in simulation, the magnetic responsive particles can then be manipulated to increase or decrease the reactance of the surface impedance based on the strength of the magnetic field present. The sub-unit cell with the greatest reactance change was then implemented into a unit cell, which is a cascade of sub-unit cells. This unit cell design was simulated, milled and tested to determine the response a unit cell should see based on extreme states of the particles represented by copper vias and open air cavities.

ACKNOWLEDGEMENTS

First and foremost, I would like to thank my committee members Dr. Daniel Ewert and Dr. Jeffery Allen, for their continued support during the duration of my research. I want to give a special thanks to my advisor Dr. Benjamin D. Braaten, for his support as well as guidance throughout my time as a student in his lab. All three of my committee members are enthusiastic about their fields and all have unique approaches to problem solving which has helped me grow as a researcher and for that I will always be grateful.

Additionally, I would like to thank my parents, Rick and Amy Cleveland, for your love and encouragement. All you've done for me, which has motivated me to pursue a higher education, has been great blessings and words cannot begin to describe how grateful I am for all you've done and sacrificed. Know that anything great I do, or will do, was because of both of you. Equally, I want to thank my sister and brother-in-law, JayCee and Levi Riehl, for always encouraging me to follow my career goals and aspirations. Also, thank you to my niece Quinn, for being a ray of sunshine on the rainy days.

My entire extended family, while numerous, has always motivated me to continue on my education and for that I will always be grateful. Specifically, I would like to thank all my grandparents for always encouraging my curiosity from when I was little and continuing to this day.

Lastly, to all my friends I could count on and who have been supportive in my endeavors, whether we saw each other daily or only occasionally, made the difference and I am sincerely grateful to have met all of you.

DEDICATION

To my amazing sister JayCee.

My greatest role model, who has always and continues to inspire me to do great things.

Through the easy and difficult parts of life, I could always count on you.

Thank you.

TABLE OF CONTENTS

LIST OF TABLES

LIST OF FIGURES

LIST OF SYMBOLS

ε_r ....permittivity, dielectric constant

f_0 ....Design frequency

c ....Speed of light, constant

k_0 ....Free space wave number

$\theta_{n=-1}$ ....Radiation angle

X' ....Average surface reactance normalized by the free-space

M ....Modulation Factor

η_0 ....Impedance, air

η_{in} ....Impedance, input

η_{sheet} ....Impedance, sheet

$\eta_{surf}(z)$ ....Impedance, surface in z-direction

CHAPTER 1. INTRODUCTION

Background

Leaky wave antennas are a traveling wave antenna that uses a transmission line structure that leaks energy along the entire length [1]. Although transmission lines typically do not radiate, a leaky wave antenna works by creating perturbed or unbalance on the line which causes the energy to radiate out [1]. The surface can be perturbed by placing vias or rectangular slots which prevents fundamental mode propagation [1]. Some of the main advantages to leaky wave antennas is the fact that they have a narrow beam width. One issue, as with many microstrip antennas, is that they need considerable modification in order to control the beam directivity. There are two categories of beam steering: frequency varying and frequency fixed. For frequency varying, some ways include designing the microstrip for a frequency varying beam [2], using changing lumped capacitance at the edge of the microstrip [3], or utilizing MIM capacitors in the design [4]. However, these methods mean they require a range of operating frequencies to work.

Fixed-frequency beam-steering can be achieved using Pin-diodes [5-7] as well as Varactor Diodes [8] and periodic via-based capacitors with digital switches [9]. For the purpose of this thesis, the method of beam steering at a fixed frequency will be the focus of the later chapters.

From the discussion of fixed frequency leaky wave antennas, a commonly shown relationship is using capacitance to vary beam directivity. One idea is that using conductive micron particles in the substrate can be used as a way to actively change capacitance between the top and bottom plane. The particles in reference are nickel-based, silver coated particles that have a diameter between 10 to 40 μm [10]. This gives them the unique property of combining and stacking to form columns following the magnetic field lines of a static magnetic field. Also, since the particles are coated in silver, the particles are conductive which leads to forming conductive

columns when a magnetic field is present. The magneto-static responsive particles have been used in structures, known as magneto-static responsive structures (MRS) which were used as a switching mechanism [11-14]. These include a switch on a transmission line [11], a switch on a filter [12] and antennas [13-14].

While the particles have been used previously as a mechanism for switching, a new approach that is explored in this thesis is how the particles can be used to create changes in the equivalent circuit of a PCB when manipulated by magnetic fields. The equivalent circuit was explored in a previous study [11] that shows the particles give a capacitive element to the circuit when placed in a substrate as a switch. Since there is a known capacitive element to having particles in substrate, and fixed frequency beam steering uses varying capacitances, using the micron-sized particles in a leaky wave design will be investigated.

Motivation for Work

Previous methods of beam steering in leaky wave antennas have been previously discussed to show that either 1) they cannot be actively tuned at a fixed frequency and 2) that actively tuned leaky wave antennas require a separate voltage. For the fixed frequency beam steering this includes Pin-diodes, varactor diodes, and digital switches. All three components require a voltage bias in order to operate the beam steering capabilities.

The magneto-static responsive particles have been researched as "binary" switches [12-14]. However, the particles have not been investigated for their response to a varying magnetic field. Utilizing the particles ability to create a capacitive element in the substrate they are located in, this thesis will investigate how a changing magnetic field could be implemented for a leaky wave antenna design.

Problem Statement

In this thesis the use of magneto-static responsive particles as an option for beam steering in a leaky wave antenna is investigated. This is explored in three ways: In Chapter 2, the mathematical and physical exploration of the leaky wave antenna is addressed. Chapter 3 utilizes a previous study on the specific perturbations cells and implementing the particles for testing, and finally, Chapter 4 concludes by comparing simulated unit cell of a leaky wave antenna to a manufactured prototype.

CHAPTER 2. CALCULATING THE SURFACE IMPEDANCE REACTANCE FOR A CHANGING GAP SIZE ON A MICROSTRIP LINE

Introduction

A leaky wave antenna can be designed as a microstrip transmission line structure which utilizes perturbations which causes the energy to "leak" or radiate along the structure [1], [14]. From the previous chapter, different methods of beam steering of a leaky wave antenna were discussed. In addition, the use of magneto-static responsive particles was also established as a novel way to magnetically controlled switch [11-14] in a purely digital sense of on and off. The purpose of this thesis is to explore integrating magneto-static responsive particles to influence beam steering based on more of an analog approach to manipulating the particles. However, to understand how an analog system with the particles would work, this thesis explores the cases of on and off for the magneto-static responsive particles.

In this chapter, the beam radiation angle of a leaky wave antenna that uses capacitive gaps as perturbations will be calculated. Additionally, the role of the capacitive gaps in the radiating field is discussed and the imaginary surface impedance derivation for a sub-unit cell using the transverse resonance technique.

Creating a Sinusoidal Chart of Reactance Values Necessary for Different Angles of Beam Radiation Based on Unit Cell Size

There are a multitude of ways to approach leaky wave antenna designs. In order to incorporate the magneto-static responsive particles, a method of designing a sinusoidally-modulated reactive surface (SMRS) was reviewed that was authored by Amit M. Patel [16]. The unique aspect of using several stages in the design process, which involved calculating the needed sinusoidally patterned surface impedances of cascaded sub-unit cells allowed for designing

4

specifically for a beam angle of radiation. The varying impedances of the connected sub-unit cells leads to a unit cell that can be repeated to form a leaky wave antenna. This approach allows for an investigation into how magneto-static particles can be used to change the surface impedances dependent on the wanted angle of radiation. The sub-unit cell and unit cell definitions are depicted in Fig. 1.
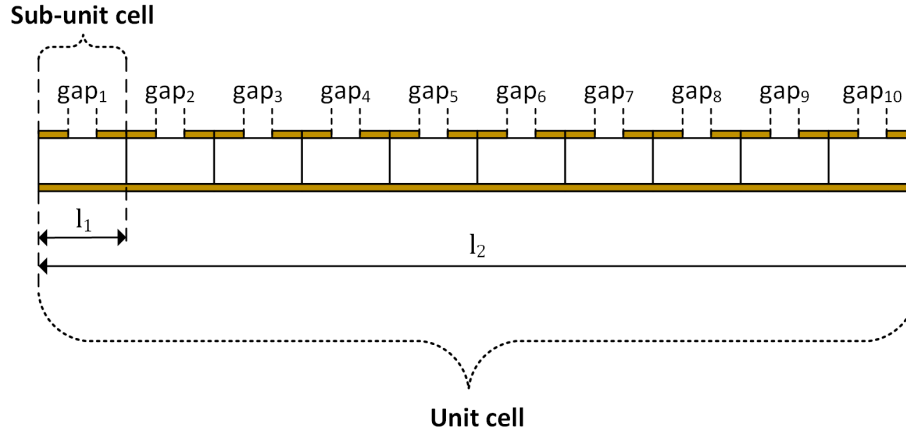
Figure 1. Diagram representation showing how a unit cell is comprised of ten sub-unit cells. Each sub-unit cell is comprised of a gap size that may be not be the same as another gap size along the line.

In order to design the unit cells, the sinusoidal variation of the radiation angle needs to be calculated. To determine the angle of radiation, $\theta_{n=-1}$ [16],

$$\sin(\theta_{n=-1}) \approx \sqrt{1 + X'^2} - \frac{2\pi}{k_0 a} \qquad (2.1)$$

can be used to calculate the angle of radiation where: a is the length of the unit cell, X' is the average surface reactance normalized by the free-space wave impedance, and

$$k_0 = \frac{2\pi f_0}{c} \qquad (2.2)$$

is the free space wave number. f_0 is the design frequency and c is the speed of light. For (2.1), the value of X' and $\theta_{n=-1}$ are unknown. From (2.1), X' can be calculated for multiple angles of $\theta_{n=-1}$ which can then be used to calculate the surface impedance

5

$$\eta_{surf}(z) = j\eta_0 X' \left[1 + M \cos\left(\frac{2\pi z}{a}\right) \right] \qquad (2.3)$$

Using the above three equations in MATLAB allows the calculations of the sinusoidally

functioned imaginary surface impedance in the z direction, $\eta_{surf}(z)$, over the length of the unit

cell a. Plotting the resulting array from (2.3), using $f_0 = 10GHz$ and $a = 28.23mm$, along the

direction of propagation, z, results in Fig. 2, which is the imaginary $\eta_{surf}(z)$ needed as the wave

propagates down the surface over the length of a in the direction of z. Additionally, in Chapter 3,

the sub-unit cell was increased to 5mmx5mm to account for a lower frequency of $f_0 = 5.8GHz$.

Therefore, $a = 50mm$ is shown in Fig. 3.

In order to find the $\eta_{surf}(z)$ values necessary for the proposed sinusoidally-modulated

surface, the sinusoid graphs of the unit cell can be divided into 10 points. Each point will become

the necessary surface impedance values for one of the 10 sub-unit cells depending on the radiation

angle which are also shown in Fig. 2 and 3 [16].
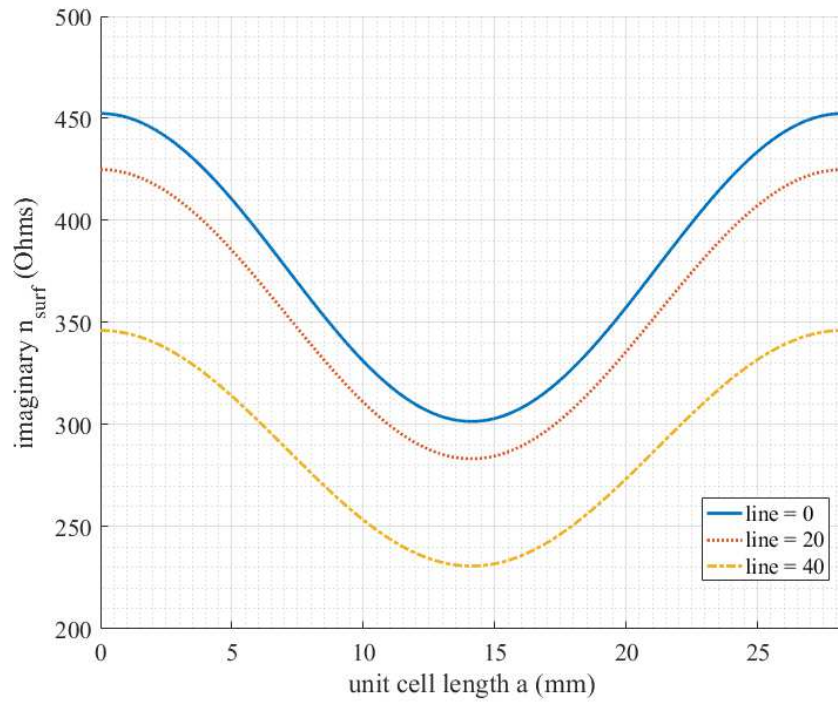
(a)
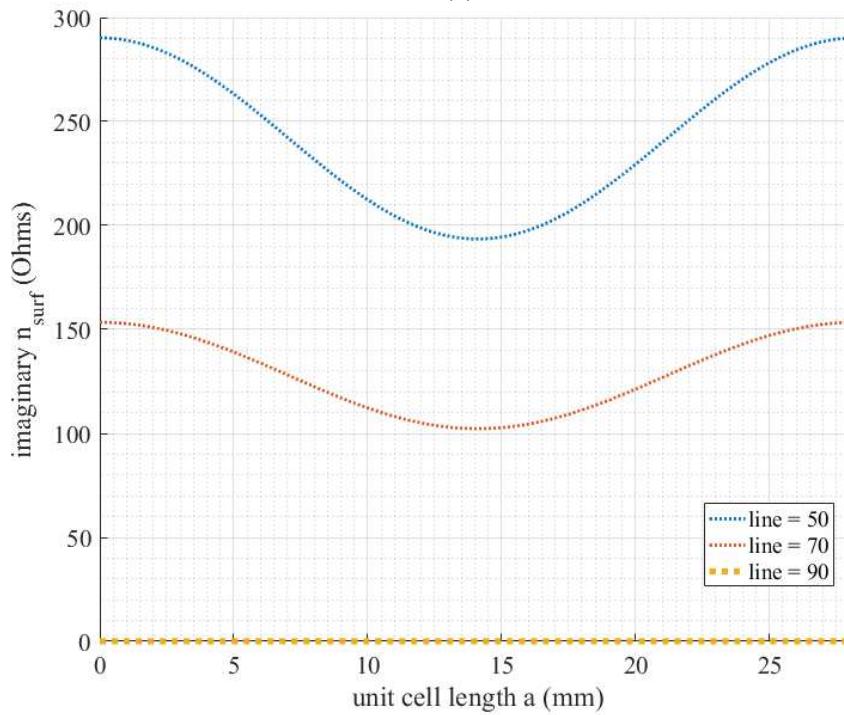
(b)

Figure 2. $\eta_{surf}(z)$ values needed for the length of a unit cell, a, at 10GHz from (a) 0 to 40° and (b) 50 to 90°.

7
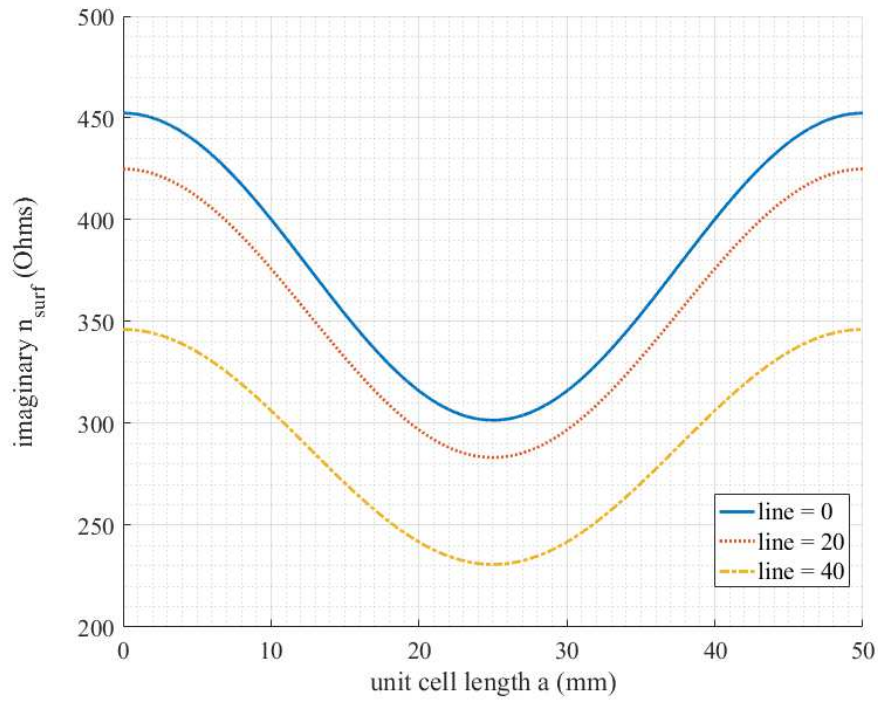
(a)
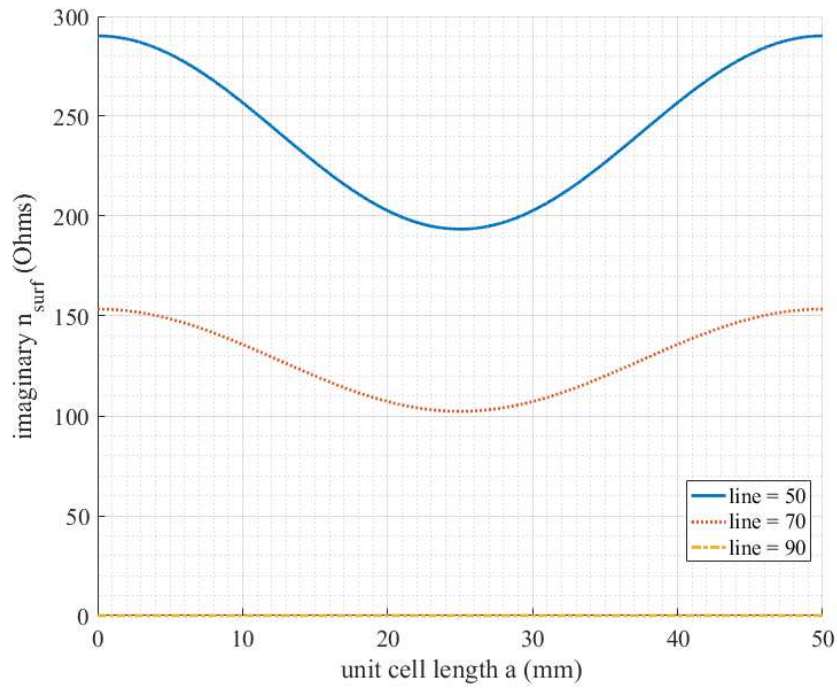
(b)

Figure 3. $\eta_{surf}(z)$ values needed for the length of a unit cell, a, at 5.8GHz from (a) 0 to 40° and (b) 50 to 90°.

Imaginary Surface Impedance Derivation of a Sub-Unit Cell and Explanation of the TRT Method

Knowing the sinusoidally modulated $\eta_{surf}(z)$ from the previous section that corresponds to different radiation angle, the changing η_{surf} will be related to a sub-unit cell model. This was done in [16] using an HFSS model to represent the transverse resonance technique (TRT) [16], which was reproduced in Fig. 4, and using only changes in the top copper piece to create a change in η_{sheet} and η_{in} which both effect η_{surf}.
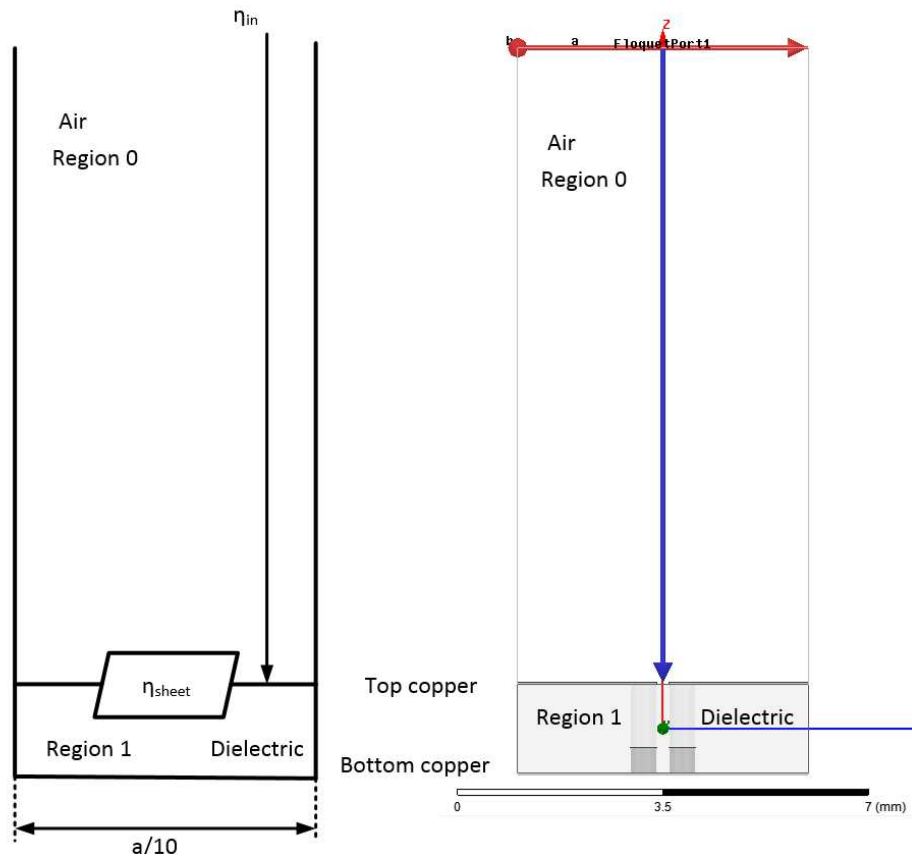
Figure 4. A Representation of how the TRT model can be represented as a HFSS model for simulation.

Relaying on the effectiveness of the TRT method, the variables line up to the represented HFSS simulation model. From Fig. 4, it can be shown that $\eta_{surf}(z)$ is a product of η_{in}, η_{sheet} and

the material properties of Region 0 and Region 1. The value of the normal incident impedance, η_{in}

is calculated from the S-parameters based on the HFSS 1-port setup shown in Fig. 4. Using

$$\eta_{in} = \eta_0 \sqrt{\frac{(1+S_{11})^2 - S_{21}^2}{(1-S_{11})^2 - S_{21}^2}} \qquad (2.4)$$

where η_{sheet} can be calculated utilizing (2.4) in

$$\frac{1}{\eta_{sheet}} = \frac{1}{\eta_{in}} - \frac{1}{j\frac{\eta_0}{\sqrt{\varepsilon_{r1}}}\tan(k_0\sqrt{\varepsilon_{r1}}d)}, \qquad (2.5)$$

where η_0 is the impedance of the air, k_0 is the wave number of air using (2.2), and ε_{r1} is the

permittivity of the dielectric between the bottom copper plate and the top copper where the gap is

located. Then using η_{sheet} and k_{x1}, the wave number of the dielectric,

$$k_{x1} = \sqrt{k_0^2(\varepsilon_{r1} - 1) + \left(\frac{\eta_{surf}k_0}{\eta_0}\right)^2} \qquad (2.6)$$

η_{surf} can be calculated using

$$\frac{1}{\eta_{surf}} = \frac{1}{\eta_{sheet}} + \frac{1}{j\frac{\eta_0 k_{x1}}{k_0\varepsilon_{r1}}\tan(k_{x1}d)}. \qquad (2.7)$$

Together using the results from (2.4) and (2.5) are used to calculate (2.6) and (2.7) using

fsolve function in MATLAB. The above four equations are necessary for determining η_{surf} for

any change in the dielectric region or change in the η_{sheet}, referring back to Fig. 4. In [16], the

author only observed how changing the gap size of a sub-unit cell creates a change in η_{sheet}. This

is where the magneto-static responsive particles integration begins. While the technique outlined

in [16] allows for designing a leaky wave antenna for one fixed frequency based on the changing

size of the gaps, it does not allow for beam steering.

The focus of the remaining chapters is in utilizing the particles to change η_{surf} when a

single fixed gap size is applied for all sub-unit cell values of η_{sheet}. From (2.5) the dielectric value

is used in the calculation of η_{sheet} and the addition of conductive magneto-static particles to the

dielectric will effect the dielectric constant of the material it is located in. Additionally, (2.6), ε_{r1} is used in calculating the wave number for the dielectric as well as also used in the calculation for η_{surf}.

Capacitive Gaps Role in Creating Radiating Fields

The effect of open-ends and gap discontinuities of microstrip lines has been reviewed in multiple papers. In [17-19], the equivalent circuit model of a transmission line gap is shown to have a capacitive effect on the microstrip equivalent circuit model. The work done in [18,19] showed the calculated capacitance created by a transmission line between the top and bottom copper conductors and the capacitance between the two edges of the microstrip lines. Fig. 5 shows how a gap in a microstrip line can be depicted as capacitances on the equivalent circuit.
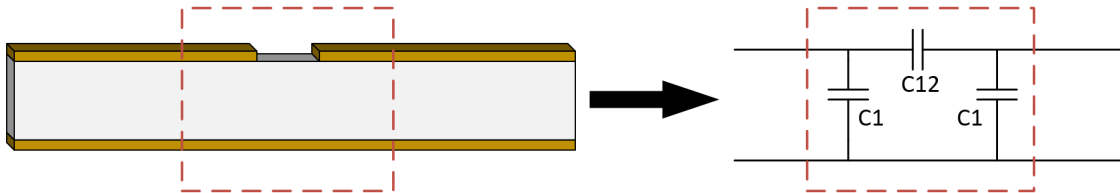
Figure 5. The gap of a microstrip line can be represented as the capacitance between the two lines (C12) and the capacitance between each line to the bottom ground plane (C1).

From [17] and [18], the capacitance of both C1 and C12 showed a relationship with the size of the gap compared to the height of the substrate. In summary, a gap that is larger than the height of substrate, C1 is greater than C12 and the opposite is true if the gap is smaller than the height of the substrate. Additionally, [17], describes how the amount of power that is leaked from the antenna is proportional to the substrate dielectric constant and the frequency, where the higher the frequency the greater the percent of power that leaves the microstrip edge at the gap.

From the review, it was shown that a gap in a transmission line can effect both the capacitance between the microstrip lines and the capacitance between the top and bottom copper.

It was also seen that introducing a gap causes energy to leak off of the line, which makes capacitive gaps in radiating fields a viable option for leaky wave antenna design. Understanding how a gap in the transmission line can lead to controlling the capacitance, both on the line and between the top and bottom copper, as well as the amount of energy lost at the gap based on frequency and dielectric of the material.

Conclusion

From the results of the sinusoidally modulated surface, it is now known the range of η_{surf} that we can use as a design requirement for the cascade of sub-unit cells that utilize the magneto-static responsive structures. In addition, the gap described on the sub-unit cell was discussed and how this gap can influence a capacitance was reviewed.

CHAPTER 3. SIMULATION BASED ANALYSIS OF CHANGING THE SURFACE IMPEDANCE REACTANCE OF A SUB-UNIT CELL BASED ON A FIXED GAP SIZE AND VARYING PARTICLES DIMENSIONS

Introduction

The use of the sinusoidally modulated surface was discussed in the previous section as a way to create a change in the surface impedance of a material. However, since the radiation pattern in [16] was determined by the physical gap sizes in the transmission line, only one radiation pattern could be designed for a single design. In this section, we will investigate the use of the micron-magneto-static responsive particle within the transmission line in order to allow for tuning the radiation of the surface, which had been mentioned throughout the last chapters.

In this Chapter, a sub-unit cell model will be created using ANSYS High-Frequency Structure Simulator (HFSS) that is used to determine the range of imaginary surface impedances. Since adding in the cavities into the design will impact the wave propagation, several different locations of the gap as well as the gaps sizes in the transmission lines were tested. Additional substrates with different dielectric constants were investigated to determine a suitable substrate that has a wide range of imaginary surface impedances depending on the state of the particles.

Model of Sub-Unit Cells in HFSS Using Floquet Ports

Based on the Transverse Resonance Technique (TRT) method discussed in the last chapter, a sub-unit cell was designed in HFSS to test the surface impedances. Since the TRT method does not account for the particles or the cavity, an approach for calculating the imaginary surface impedance included two different HFSS simulations: The first is used to recreate the TRT method on the sub-unit cell called the 1-Port model and the other, called the 2-Port model, is used to

calculate the dielectric permittivity (ε_r) of the substrate with the cavity of air and the particles simulating both with and without the magnetic field.

For the 1 Port model, the dielectric with air cavities and particles are tested with the top and bottom copper planes. The top plane has a gap in the copper which was built off of the design from [16] which creates the increase in surface impedance which allows the energy to leak from the transmission line. The port, a floquet port with master/slave boundary conditions as described in Fig. 6, was placed a distance of four times the substrate heights away from the surface of the top copper plane. Varying the gap on the top layer of copper is what was studied in [16] as a method of changing the surface impedance of the leaky wave antenna. When testing the surface impedance of one configuration of air cavities, the particles were tested in their two states: with and without magnetic fields, as shown in Fig. 7.

Top

Bottom

Figure 6. The 1-Port HFSS Boundary (Top) and excitation (Bottom) set ups for the sub-unit cell testing.
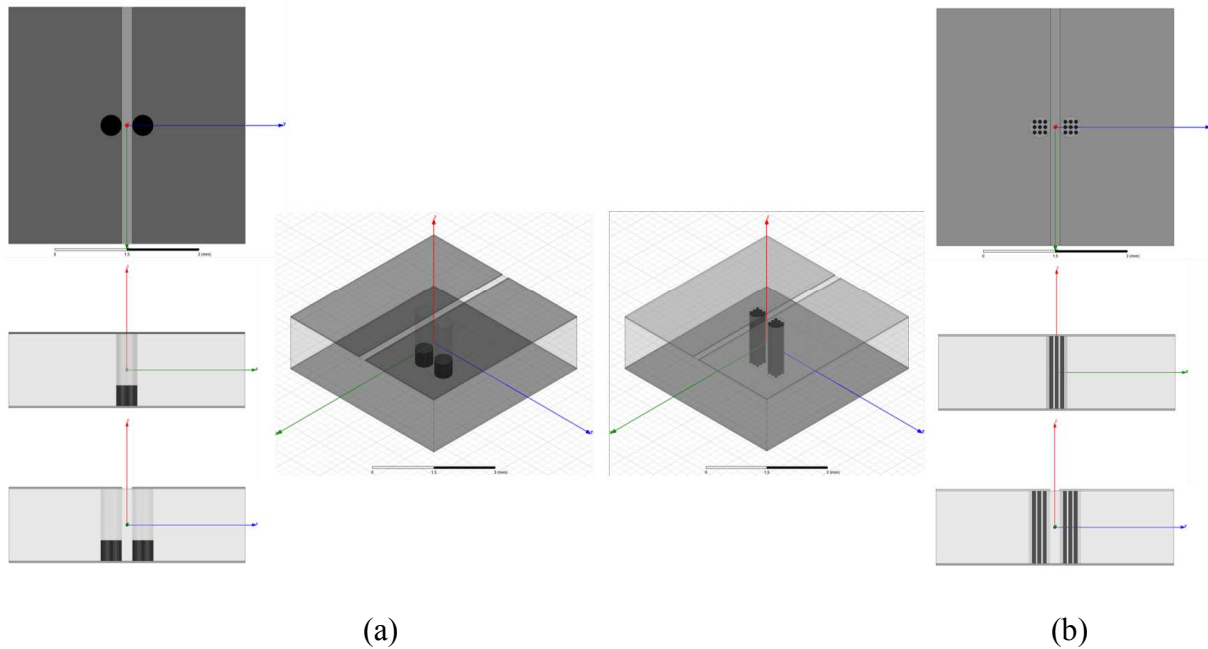
Figure 7. Multiple views for the 1-Port HFSS Models of (a) without magnetic fields and (b) with magnetic fields present for sub-unit cell testing.

Next, the 2-Port model simulation of the dielectric with the cavities are done with two floquet ports. This allows for the surface of cavities and particles to look electrically large. The ports are set three substrate heights away on both sides and were de-embedded within the MATLAB code that calculates the permittivity of the dielectric. The model ports and boundaries setup is shown in Fig. 8. For each 1-port model, shown in Fig. 7, the dielectric 2-Port test is run in order to know the change in the dielectric permittivity that changes depending on where the particles are in the cavities. The different test setups are shown in Fig. 9.
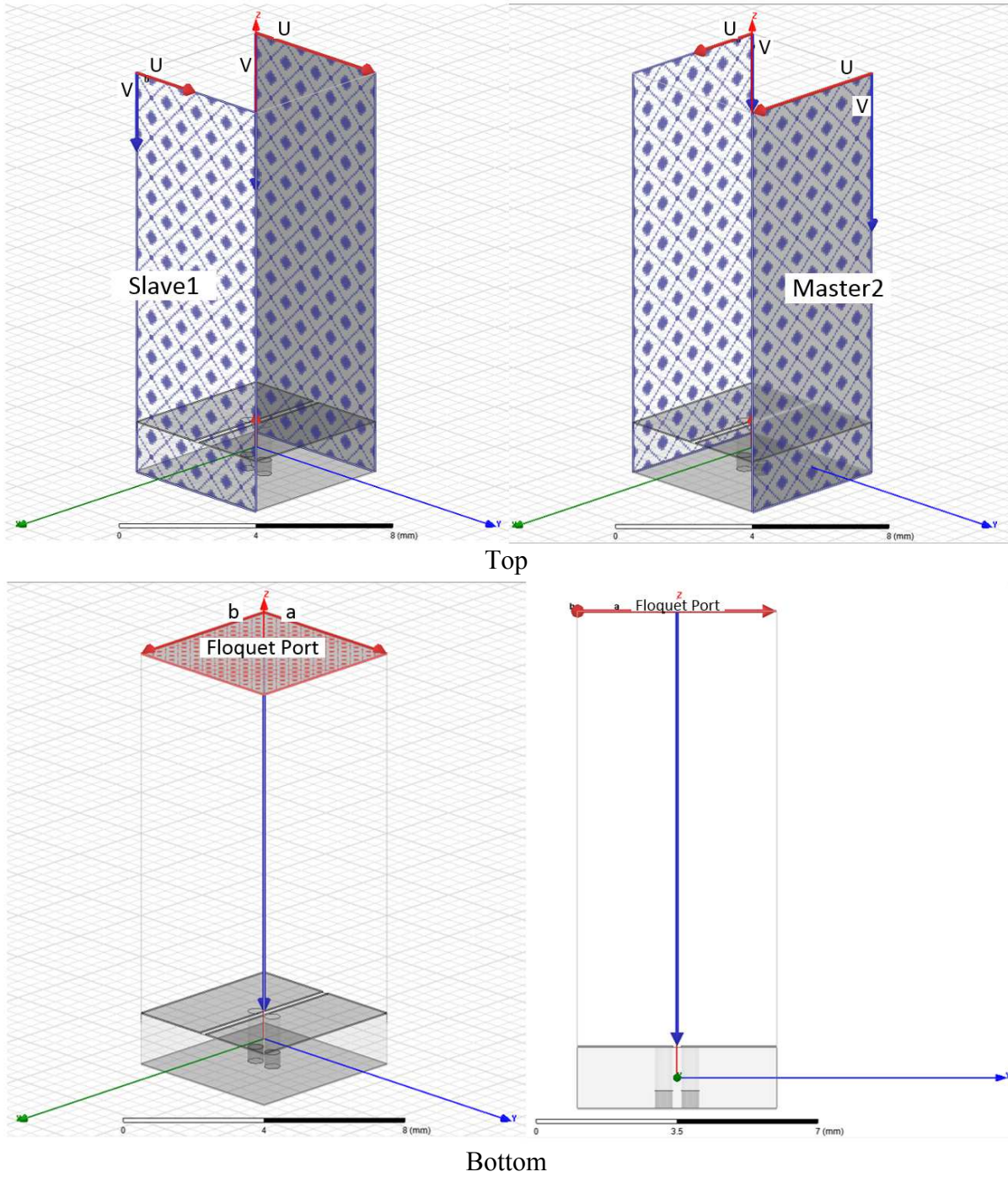
Top

Bottom

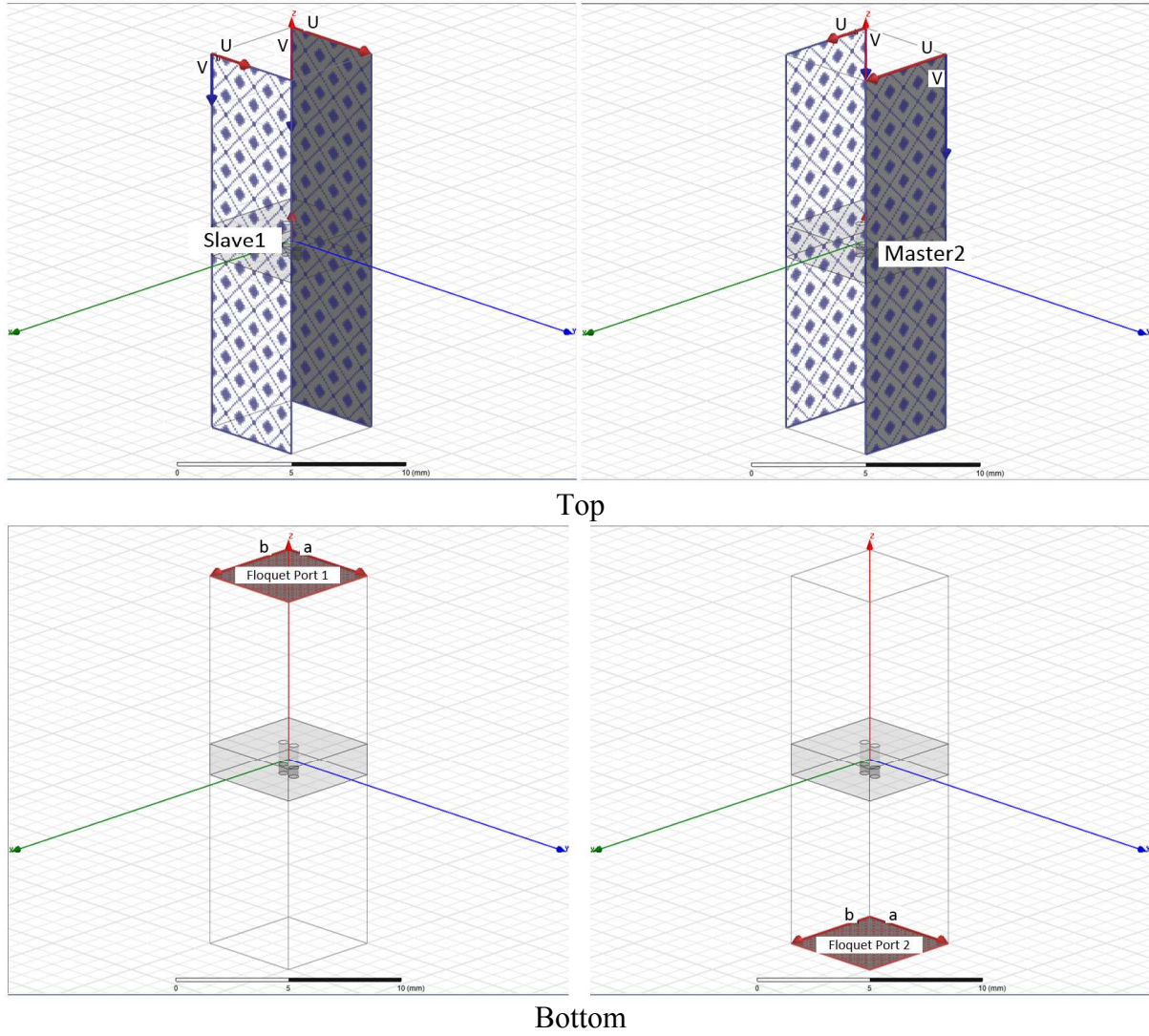Figure 8. The 2-Port HFSS Boundary (Top) and Excitation (Bottom) set up for the sub-unit cell testing.
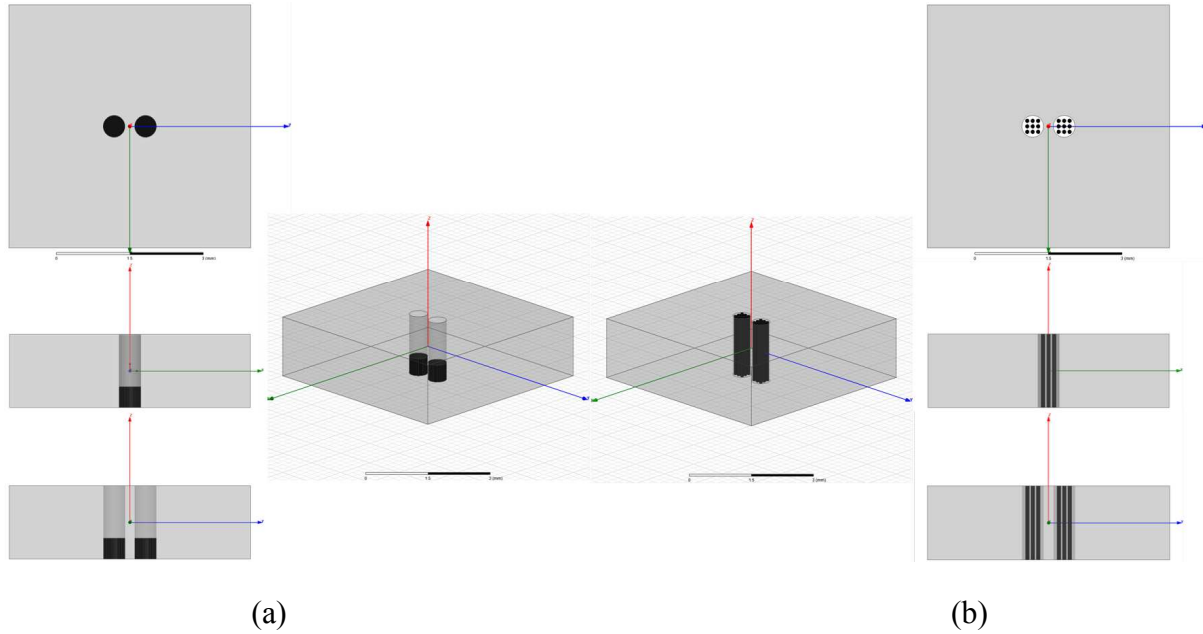
Figure 9. Multiple views for the 2-Port HFSS models of (a) without magnetic fields and (b) with magnetic fields present for sub-unit cell testing.

Having the results of the two HFSS simulations for each of the states of the particles, it is then possible to calculate the imaginary surface impedance η_{surf} of the sub-unit cells, which was outlined in Chapter 2. Using the results of the dielectric simulations the S-parameters were used in a MATLAB code to calculate the permittivity and permeability of the dielectric slab. Once the dielectric value was calculated, the permittivity and permeability were used in the formulas in Chapter 2 to calculate the imaginary surface impedance η_{surf} based on the S11 retrieved from the 1 port test.

Simulation of Different Configuration of Cavities

The following simulations were ran using a substrate of Arlon AD600 (εr =6.15 and tan δ=0.003) at a frequency of 10 GHz. To start, the modeled substrate and frequency were used based on the work done in [16] which only used a changing gap size pattern as the way to design a surface with a changing imaginary surface impedances. In the following two experimental setups, the goal

was to explore how the placement of the particle containing cavities manipulated the imaginary surface impedance. The experimental sizing of the sub-unit cell is in Fig. 10.
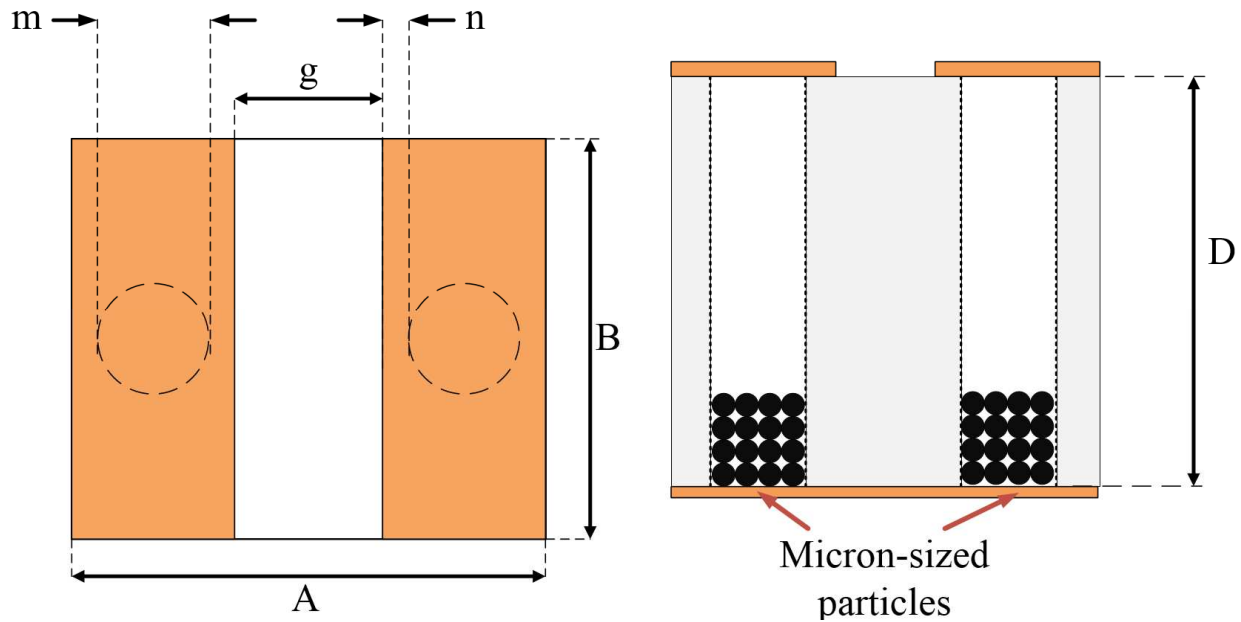
Figure 10. A drawing of the sub-unit cell taken from [21] which describes the dimensions and variables. For the following tests for Arlon AD600 and frequency of 10GHz: m = 0.45mm A = B = 2.86mm and C = D = 2.54mm. The gap, g, and distance of the cavity to the edge of the gap, n, will be varied in the next sections.

Two experiments for the sub-unit cell were devised for testing the variables Gap and n from Fig. 10. The first was to vary the size of gap, g, while maintain a fixed size of n. The second was to use a fixed size of g and investigate the changing value of n, which relates the distance from the nearest edge of the cavity to the gap. The following two experimental design in HFSS and results are discussed.

Movement of the Gap

The changing size of the gap size, g, on the top transmission line, when no substrate cavities or magneto-static particles are present, was explored in previous work [16] which designed a sinusoidally modulated reactive surface. The range of imaginary surface impedances seen in [16] work was used as validation to determine if changing the state of the particles in cavities could

cause a similar range of imaginary surface impedances when the gap size was fixed in a sub-unit cell model. For the simulation, a sub-unit cell was designed as discussed in the previous section.

The variable g on the top copper layer was varied from 0.2mm to 1.8mm. The cavities were held at n = 0 during the Optimetrics solutions. In addition to the 1-port floquet Optimetrics test, the 2-port dielectric simulation for all five values of g, also shown in Fig. 11. All ten tests show in Fig. 11 were performed for both with magnetic fields present and without magnetic fields present.
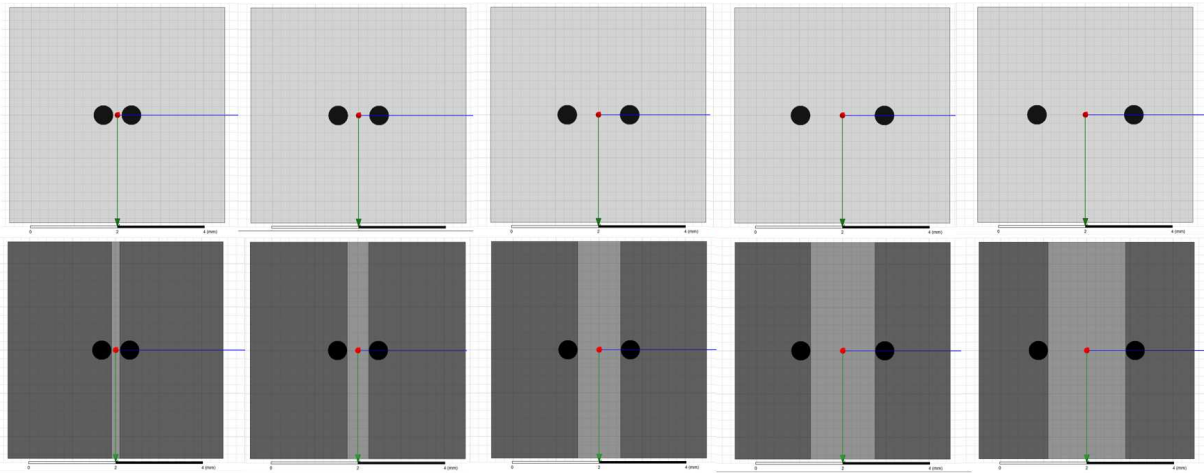
Figure 11. The variation of g for the 2-Port test (Top) and 1-Port test (Bottom) while n = 0 for g = (a) 0.2mm, (b)0.5mm, (c) 1.0mm, (d) 1.5mm, and (d) 1.8mm.

Movement of Cavity in Relationship to the Gap

With a fixed gap size of g = 0.5mm, the values of n, referencing Fig. 10, is varied from 0mm to 0.6mm. This was done to determine if the location of the cavity of particles in the sub-unit cell had a pronounce difference in changing the imaginary surface impedance. The 1-port setup and the dielectric 2-port simulations are shown in Fig. 12, depicting varying n effect both models. All of the 1- and 2-Port simulations were set with an Optimetrics that that moved the location of the cavities for the five values of n that were tested.
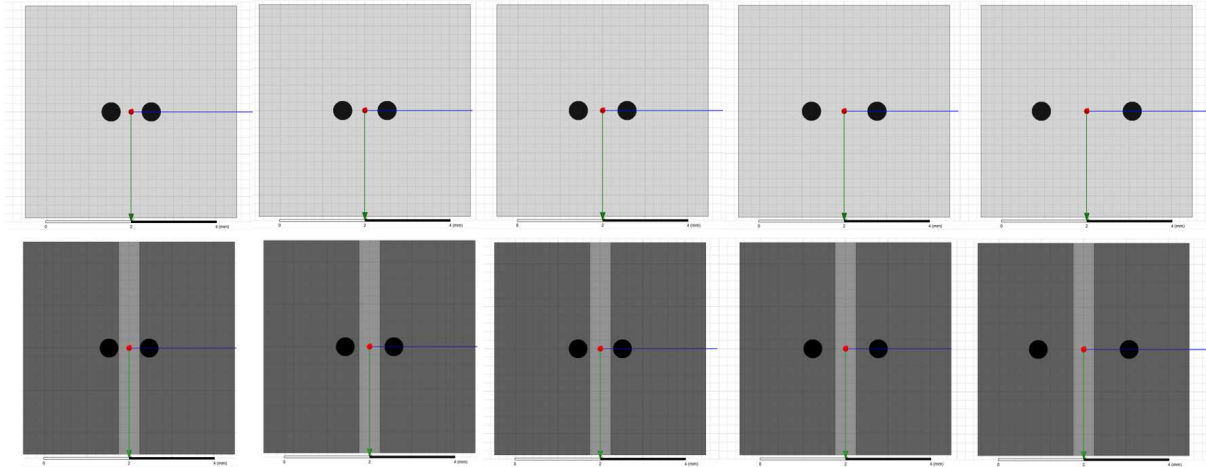
Figure 12. The variation of n while g = 0.5mm for n = (a) 0mm, (b) 0.05mm, (c) 0.1mm, (d) 0.3mm, and (e) 0.6mm.

Results

Using the 2-Port simulation cases shown in Fig. 11(Top) to calculate the dielectric permittivity the substrate, the values of the 1-port simulations are shown in Fig. 13. The results showed that as the gap size, g, decreased, the change in surface impedance from the two states of particles increased considerably. This also showed that when no Magnetic field is present is where the size of the g had the most effect on changing the imaginary surface impedance value. Included in the results is the validation test where the cavities and particles were not present. The validation line was based on the setup in [16] for sub-unit cells to show that this simulation model and setup were comparable to previous work.
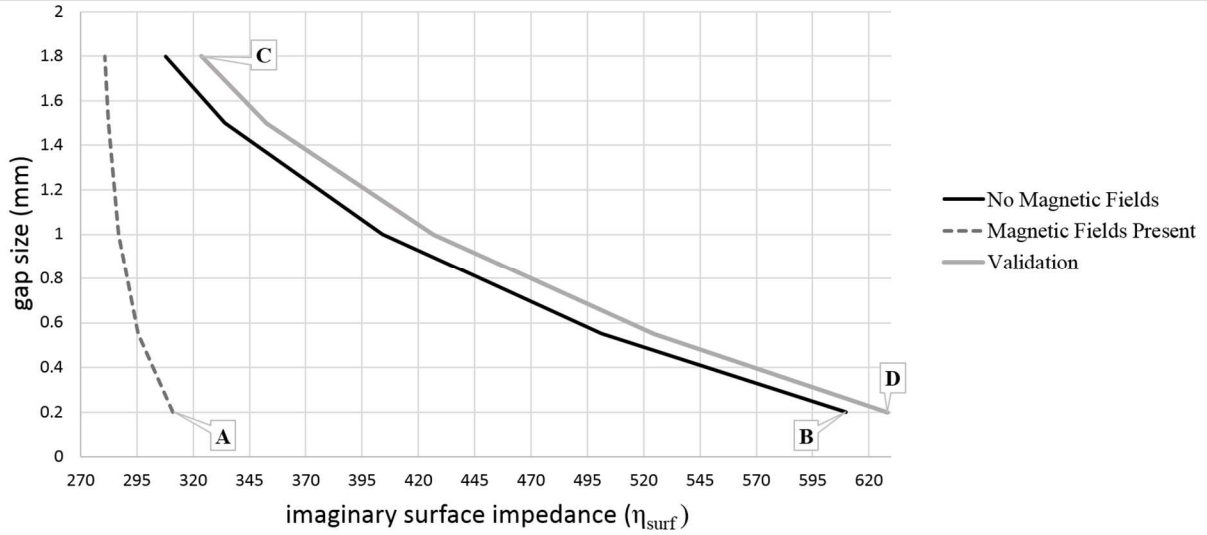
Figure 13. Results from different values of varying g = 0.2 to 1.8mm when n = 0 for the tested: No Magnetic Fields, Magnetic Fields Present, and the validation [16]. [22]

The dialectic simulations cases shown in Fig. 12 Top were used to calculate the dielectric permittivity of the substrate used for the 1-port simulations are shown in Fig. 12 Bottom. The results are shown in Fig. 14. While the gap, g, was held at 0.5mm, the value of n was changed. For the results, the change in the value of the imaginary surface impedance had the greatest variation when the distance of n from the gap was at zero. The effect on the placement of the cavity had a greater effect on the test case with magnetic field present.
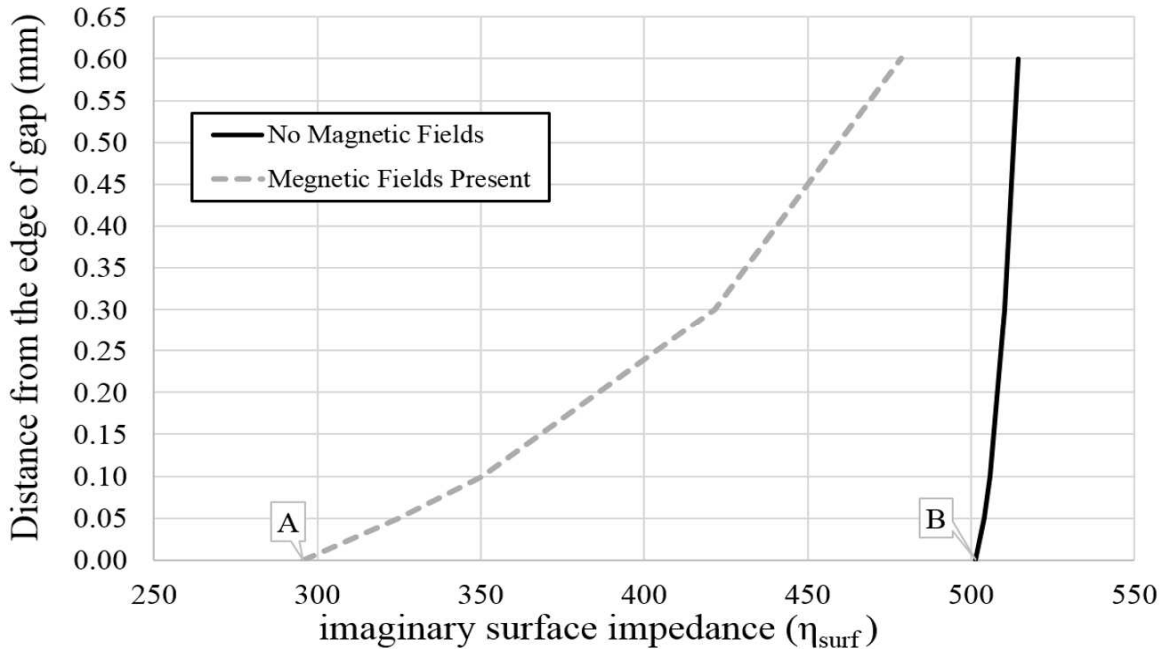
Figure 14. Results from different values when varying n=0 to 0.6mm when g = 0.5mm for No Magnetic Fields and Magnetic Fields Present. [21]

From the results of the sub-unit cell tests described above, comparing how the size and placement of g and n in the sub-unit cell, shows variation of imaginary surface impedance from the case with the magnetic fields present and without magnetic fields. The results of these tests were considered for the final case of the sub-unit cell involving choosing a new substrate to test.

Testing Additional Substrates for Use at 5.8GHz

Knowing how gap size and location of the particle-containing cavities results in ranges of imaginary surface impedances based on magnetic fields, the objective now was to design a sub-unit cell that matched the design goals outlined in Chapter 2. This being a sub-unit cell that worked at 5.8GHz and used a Rogers TMM substrate.

One thing that was noticed during testing was that once the frequency was dropped on the sub-unit cells shown in previous tests, the impedances changed significantly and testing with a unit cell of that size was no longer feasible. The unit cell was changed to be a quarter wavelength of

23

our operating frequency 5.8 GHz. Therefore, the unit cell was increased to A = B =5mm, in reference to Fig. 10, for the TMM testing described below.

For the Rogers TMM tests, TMM4 and TMM10i were tested which has a dielectric constant of $\varepsilon_r = 4.5$ and $\varepsilon_r = 9.9$, respectively. This was tested to see how ε_r played a role in changing the imaginary surface impedance. The 2-Port and 1-Port tests described earlier in the chapter was used for these tests. Table 1 shows the results of the different TMM substrates that were tested.

Table 1. Comparing two different Rogers TMM substrates, tested as sub-unit cells at 5.8 GHz with a sub-unit cell that is 5x5mm.

Rogers TMM name	Height (mm)	2-port test (ε_r)		1-Port test (imaginary impedance) Ω	
		Magnetic Fields Present	No Magnetic Fields	Magnetic Fields Present	No Magnetic Fields
TMM4	1.52	4.459	4.515	31.00	132.26
TMM10i	3.18	9.651	9.797	475.31	914.66
TMM10i	1.52	9.653	9.812	42.47	653.20

From the results shown in the figure above, it shows that TMM10i (ε_r =9.9 and tanδ = 0.0020) at 5.8GHz shows a range of 610.73Ω for the imaginary surface impedances between Magnetic Fields Present and No Magnetic Fields. Based on sub-unit cell testing, Rogers TMM10i with a height of 1.52mm was chosen for further design for the unit cells explored in Chapter 4.

Conclusion

When designing a sub-unit cell for use in additional unit cells, three variables were simulated to determine a configuration that was best suited for multiple unit cells: 1) size of gap, 2) location of cavity in the dielectric in relation to the gap, and 3) the height and type of substrate used. All three were investigated and the findings were compared to multiple samplings. First, it was shown that using the cavities in the dielectric as the method of changing the surface impedance showed the best change in imaginary surface impedances when the gap was the smallest at g =

0.2mm. Next, the location of the cavities in the dielectric were shown to provide the most influence on the imaginary surface impedance when the cavities' outer wall was located at the edge of the gap but did not merge into the gap. Finally, different substrates were tested to determine at what height and dielectric constant gave the best results for changing the imaginary surface impedances.

Now that multiple variables have been determined with the sub-unit cell testing, a unit cell matching the best cases of the three tested in this chapter was created in simulation, manufactured into physical models, and compared in the next chapter.

CHAPTER 4. SIMULATING AND MANUFACTURING A UNIT CELL MODEL BASED ON THE SUB-UNIT CELL

Introduction

From the previous chapter, sub-unit cells were designed and simulated to show how two states, no magnetic fields and magnetic fields present, can affect the surface impedance of a sub-unit cell. The data gathered showed the necessary dimensions for each sub-unit cell to be a single gap size, g, and for the distance of the cavity from the edge of the gap, n, for all sub-unit cells. The finalized dimensions are shown in Fig. 15. The unit cell, which consists of 10 sub-unit cells, were designed based on the results of the previous chapter. In this Chapter, two unit cells designs, open cavity and copper vias, were tested using simulation software and compared to milled prototypes.

HFSS and ADS Model Creation and Setup

The unit cell models were based on connecting 10 sub-unit cells together, which were explored in the previous chapter. From the previous chapter, it was concluded that having a gap size, g, of 0.2mm while having the cavities of the particles located at n = 0mm showed the greatest variation in surface impedances mapped out in Fig. 15. However, due to milling and via availability, the vias were increased from a diameter of 0.45mm to 1.0mm, while g = 0.5mm and n = 0.1mm were used with the substrate TMM10i (ε_r = 9.9 and tanδ = 0.0020) which had a thickness of 1.52mm. Also, the width of the unit cell was increased to 7.22mm to allow for the larger via. In this chapter HFSS as well as Advanced Design Systems (ADS) were used to simulate the unit cell design.
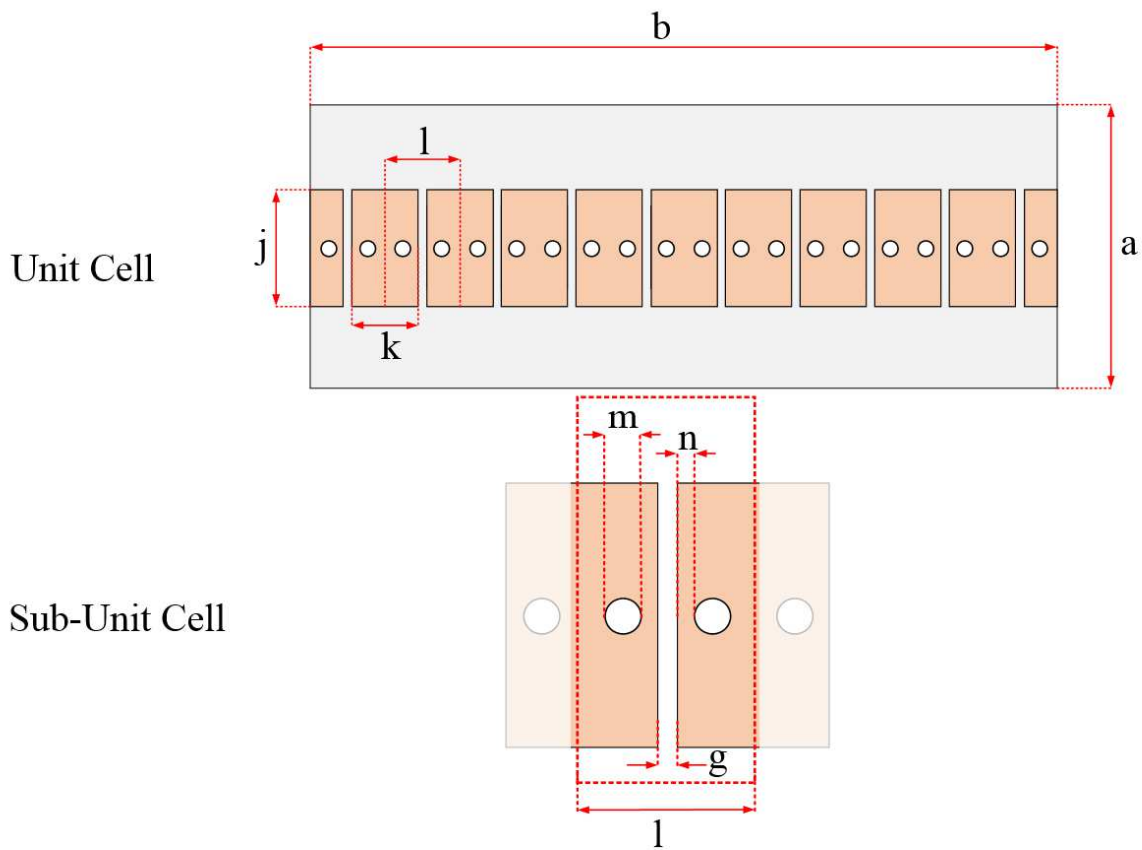
Figure 15. Modified unit cell dimensions based off of sub-unit cell testing from last chapter. a = 30mm, b = 60mm, g = 0.5mm, j = 7.22mm, k = 4.5mm, l = 5.0mm, m = 1.0mm, and n = 0.1mm. Note that m is the diameter of the hole for the via and n is the distance of the cavity from the edge of the gap, g.

For the HFSS simulation setup, two lumped ports were used at the ends of the unit cell in Fig. 16 and 17 the radiation box was 60x120x70mm and had the unit cell centered inside. The analysis setup included a sweep of frequencies from 4 to 8GHz, with the solution frequency of 5.8GHz, Max passes of 20 and Max Delta S of 0.05. Two designs were created: open cavity, Fig. 16, and copper via, Fig. 17. These two cases were used to show the extreme possibilities of having particles in the cavities. However, for the beam steering discussed previously, each sub-unit cell of a unit cell would have a separate imaginary surface impedance from the adjacent sub-unit cells. This means all adjacent locations would have particles effected by different intensities of the magnetic field. Further work on controlling the particles is discussed in Chapter 5.

27
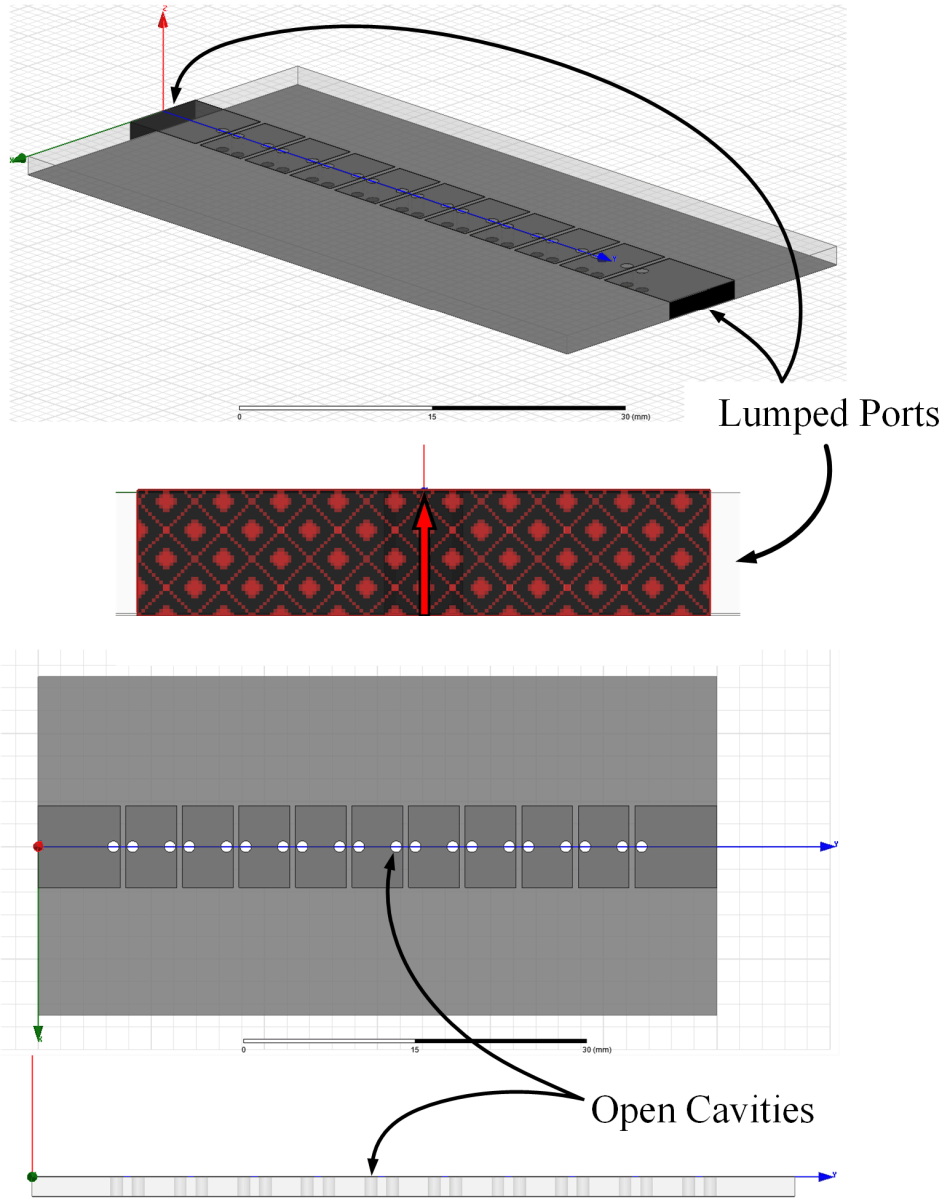
Figure 16. HFSS unit cell for the open cavities case, showing the lumped ports and cascading sub-unit cells.

Figure 17. HFSS unit cell for copper via case that includes the lumped ports and cascading sub-unit cell.

ADS Simulation Setup

In ADS there are a few differences in designing the model than in HFSS. First, ADS is all 2-D design, making the substrate and via declaration important. Additionally, the ports in ADS are point sources and required a line extension in this case, which is shown in Fig. 18. For ADS, the

case for copper vias was the only model simulated due to momentum's inability to simulate non-conductive vias.

Manufacturing of Unit Cells Based on Simulations

For the two cases described previously in this chapter, open cavities and copper vias, a unit cell model was printed and tested. Using an LPKF S63 milling machine, the prototypes were milled and assembled using edge mount SMA connectors. Additionally, LPKF Easy Contac copper vias of 1.0mm were utilized for the copper via case. The two assemblies are shown in Fig. 19.
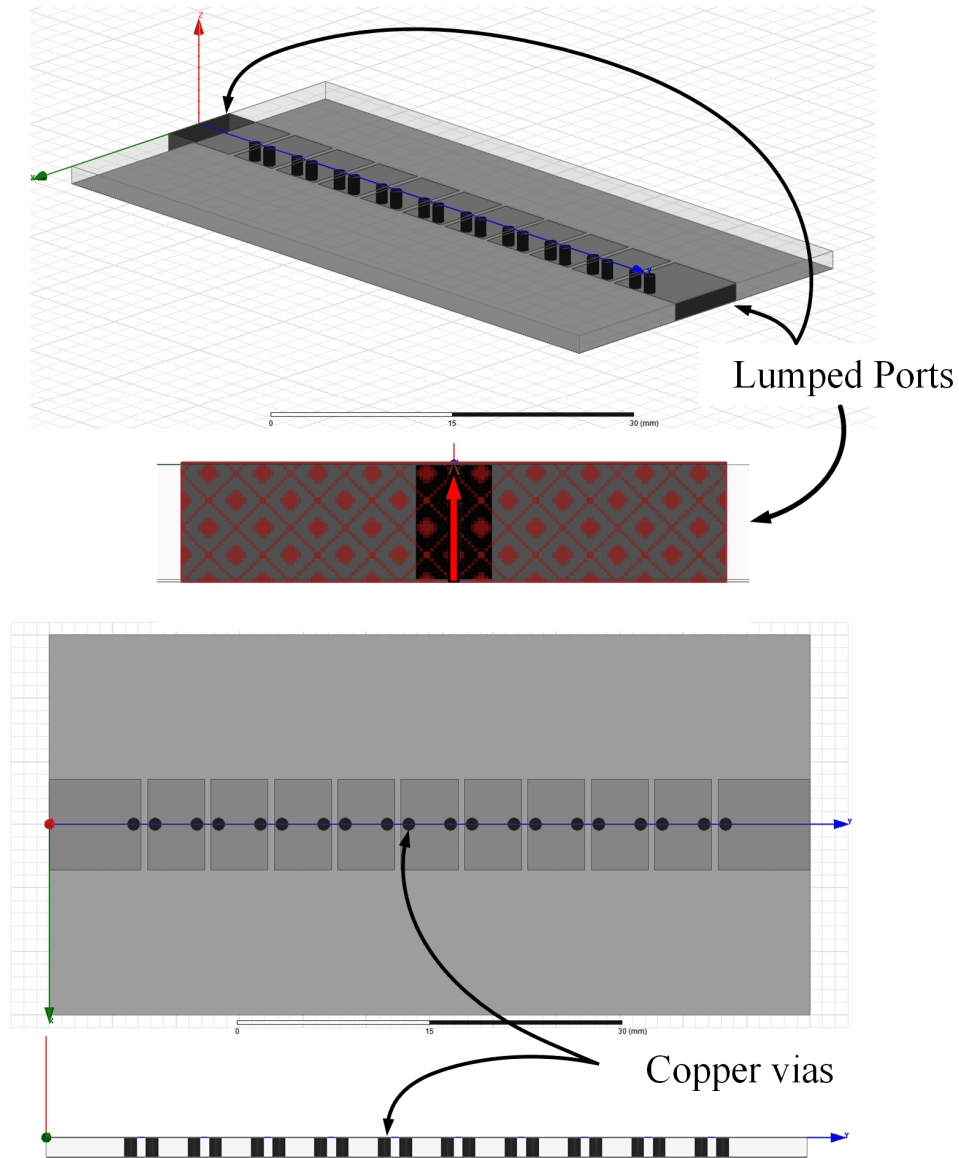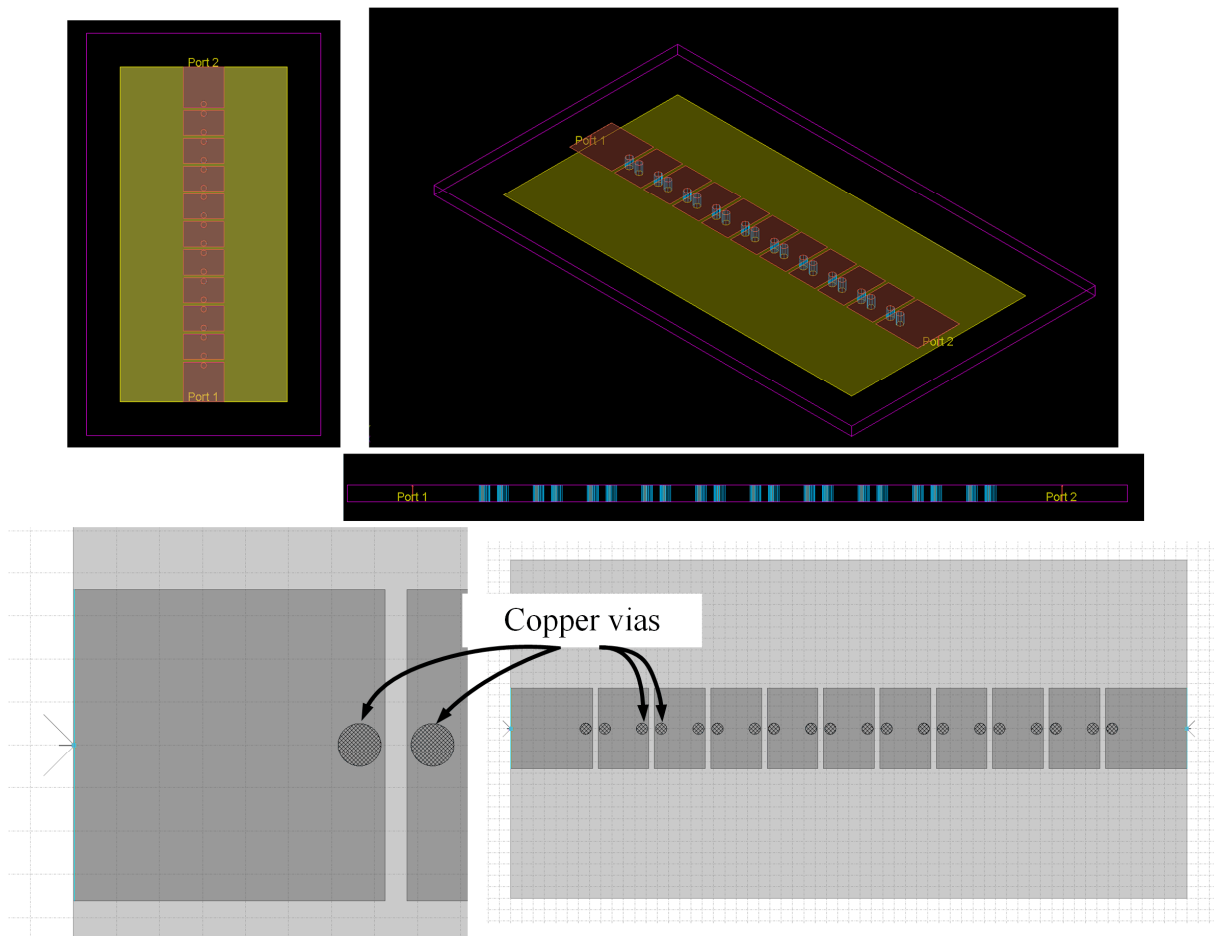

Figure 18. ADS unit cell setup for copper via case. Including ports and cascading sub-unit cells.

Figure 19. Prototype of the unit cell design for the open cavity case (left) and the copper via case (right).

The two manufactured unit cells were tested using a Keysight E5071C ENA Series Network Analyzer 100kH – 8.5GHz.

Results of Simulations and Prototypes

In Fig. 20, the design with air cavities is shows that for at design frequency of 5.8GHz, the prototype had an S21 value of -25.5 dB and the HFSS model had a value -23.6 dB.

From Fig. 21, the design with the copper vias, it shows that the prototype had an S21 of -34.44 dB, HFSS S21 was -48.0, dB and ADS S21 was -37.3dB for the design frequency of 5.8GHz.

For the copper vias case, the HFSS simulation showed a sharp decrease from 5.6 to 6GHz, which similar responses were seen in the ADS simulation as well as the prototype measurement at different frequencies. However, although the S21 measurements for the copper vias case were not as close as those of the air cavities, all three copper via measurements show at least a drop of 8.9dB or more from the case of air cavities.

31
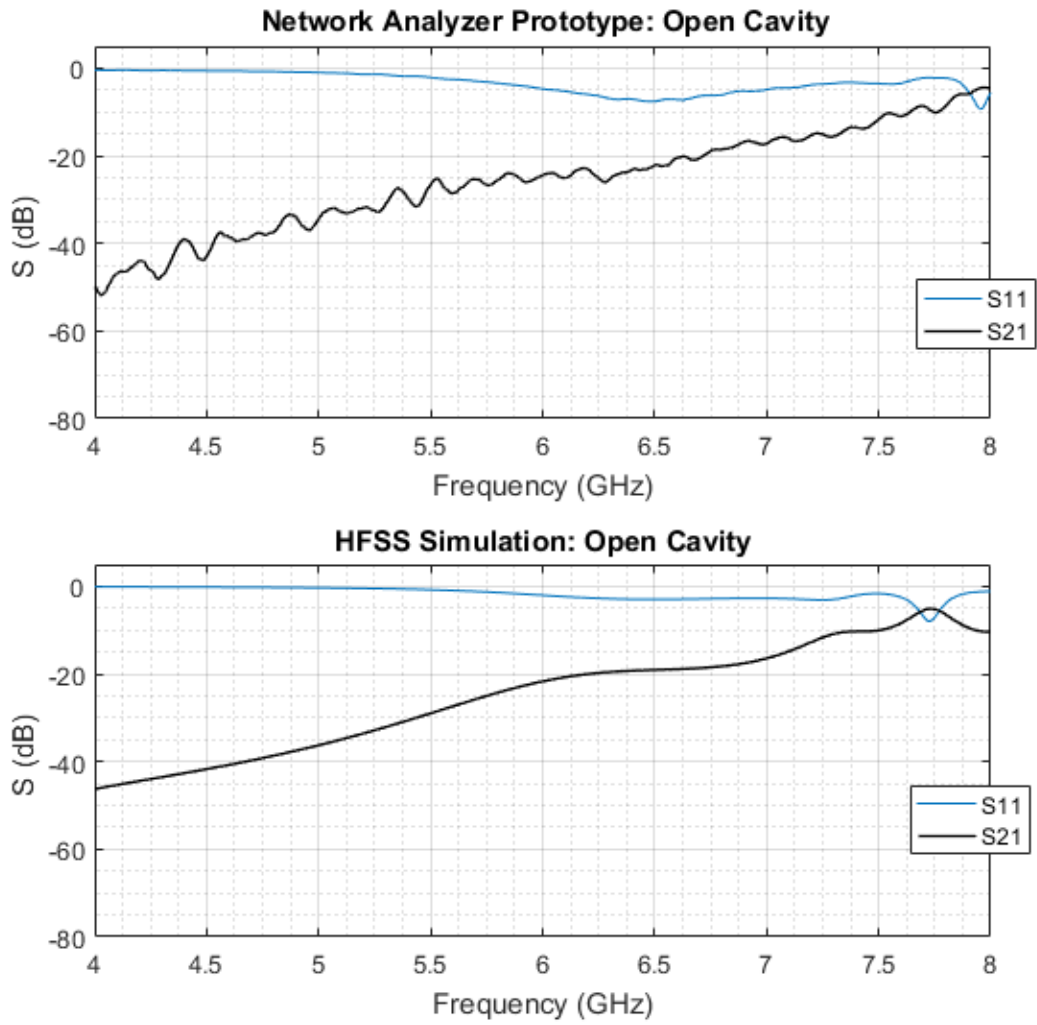
Figure 20. Open Cavity Network Analyzer and HFSS results.
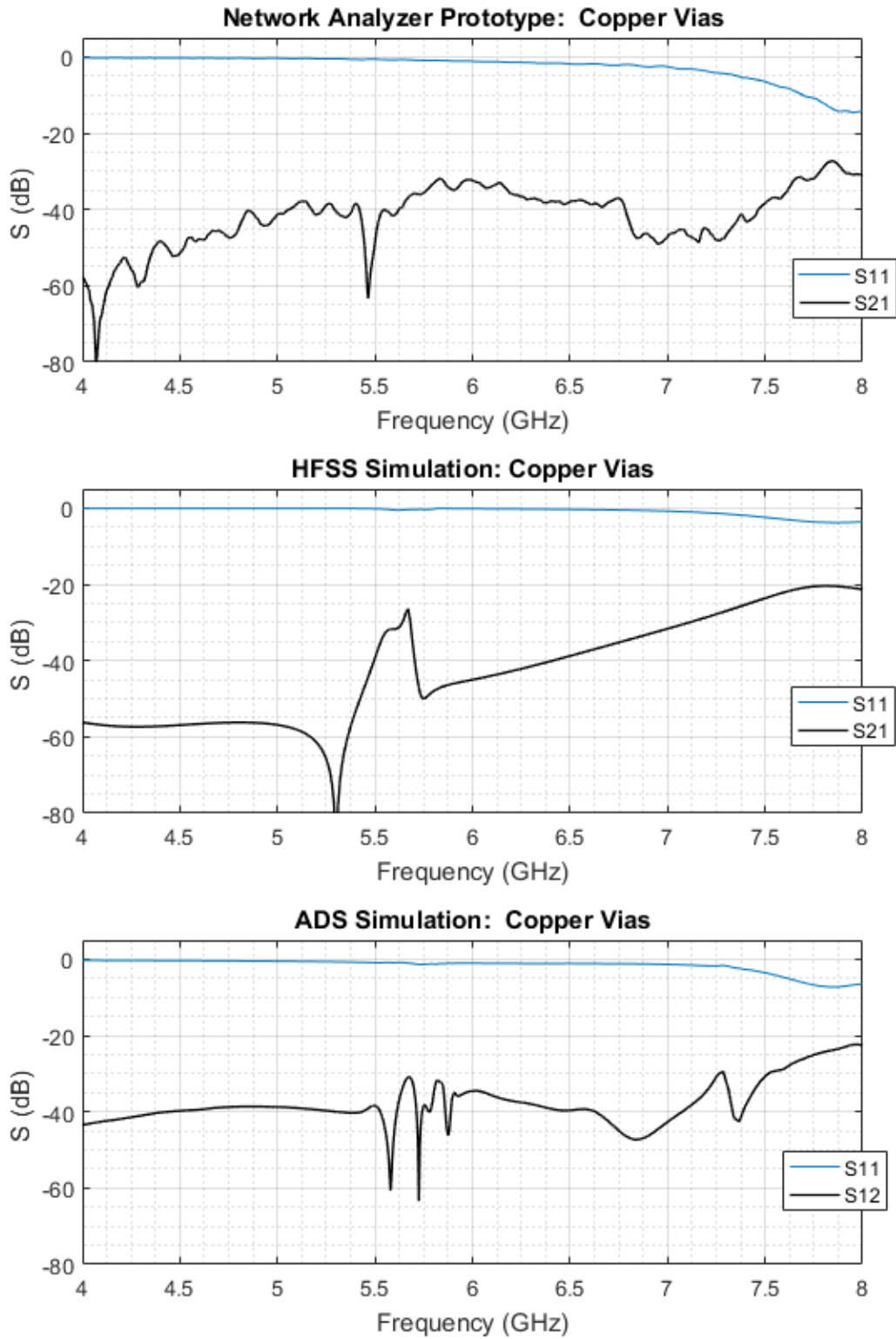
Figure 21. Copper via using Network Analyzer, HFSS, and ADS Results.

Conclusion

A unit cell designed for a leaky wave antenna was created which used two types of cavities, copper vias and air cavities, to effect S-parameters. This is possible as a gap in a microstrip line will create capacitances in two ways: first, between the two copper lines that are split and second both edges of the gap with the bottom copper layer. From the results, the matching between the S-parameters gathered through HFSS, ADS, and prototypes show a good correlation between both simulated S-parameter and prototype measurement. Between the air cavities and copper vias it was shown that the S21 for the copper vias dropped by at least 8.9 dB when compared to the air cavities. This shows that the copper vias had a decrease in the amount of power being transmitted from port 1 to port 2 compared to the air cavities case.

CHAPTER 5. FUTURE WORK AND CONCLUSIONS

Future Work

While this thesis explored the magnetic field in two states, Magnetic Fields Present and No Magnetic Fields, further research into how to vary the control of the magnetic fields to manipulate the sub-unit cell models seen in Chapter 3 is needed to implement the particles in the full transmission line design. This further research would help to show how to achieve the varying imaginary surface impedances shown between the two extreme cases, with magnetic fields and without magnetic fields present, to allow for beam steering, which was explained in Chapter 1. This would be possible by investigating the particles' responses to varying the magnetic field strength in a controlled setting. Once it is established how varying the magnetic field strength influences the imaginary surface impedances, a full leaky wave antenna design based off of the sub-unit and unit cell models discussed in this thesis may be created. Lastly, future studies in the geometrical design of the cavities would provide additional insight into the effects of the particles based on placement to control the surface impedance. This would include using different, non-cylindrical shapes such as cones and rectangular cavities to place the particles between the top and bottom copper planes.

Conclusions

This thesis has covered multiple topics, including the design, calculation and implementation of a modulated surface impedances to control the angle of radiation. The motivation behind the work was to create a method of using micron-sized, magneto-static responsive particles as a way to vary the surface impedances of a sub-unit cell. The potential for active tuning the particles lead to these ideas explored in previous chapters. Furthermore, an existing method of designing a sinusoidally modulated reactive surface was adapted to allow for

addition of cavities containing particles using changing orientation as a way to change the reactive surface impedances.

Additionally, the exploration of how systematic gaps in a microstrip line can be used together with cavities containing micron-sized, magneto-static responsive particles was evaluated through sub-unit cells using HFSS. From these test, it was determined that the size of the gap of a sub-unit cell as well as the distance of the cavity from the gap played a role in the values of the imaginary surface impedances for when a magnetic field was and was not present for the particles.

Using the dimensions determined from previous tests, two prototypes were milled and tested against electromagnetic simulation software models to determine if the presence of the vias or air cavities created a noticeable change. Since a noticeable change was shown between the results of the two states' S-parameters, for both prototype and simulation models, the results help to predict that implementing micron-sized particles into the unit cell design will also show a noticeable change in the S-parameters, which will be explored in future work. From the results throughout this work, the fundamentals of how micron-sized, magneto-static particles could be used successfully with a periodically gapped microstrip line to change the reactive surface impedance.

REFERENCES

[1]   W.L. Stutzman and G.A. Thiele. *Antenna Theory and Design,* 3rd ed. Hoboken, NJ: Wiley, 2013, pp. 481-483.

[2]   Y. Weitsch and T. F. Eibert, "Continuous Beam-Steering Leaky-Wave Antenna based on Substrate Integrated Waveguide," *The Second European Conference on Antennas and Propagation*, EuCAP 2007, Edinburgh, 2007, pp. 1-5.

[3]   M. Archbold, E. J. Rothwell, L. C. Kempel and S. W. Schneider, "Beam Steering of a Half-Width Microstrip Leaky-Wave Antenna Using Edge Loading," in *IEEE Antennas and Wireless Propagation Letters*, vol. 9, pp. 203-206, 2010.

[4]   H. V. Nguyen, S. Abielmona, A. Rennings and C. Caloz, "Pencil-Beam Full-Space Scanning 2D CRLH Leaky-Wave Antenna Array," *2007 International Symposium on Signals, Systems and Electronics*, Montreal, QC, 2007, pp. 139-142.

[5]   Y. Geng, J. Wang, Y. Li, Z. Li, M. Chen and Z. Zhang, "Radiation Pattern-Reconfigurable Leaky-Wave Antenna for Fixed-Frequency Beam Steering Based on Substrate-Integrated Waveguide," in *IEEE Antennas and Wireless Propagation Letters*, vol. 18, no. 2, pp. 387-391, Feb. 2019.

[6]   D. K. Karmokar, D. N. P. Thalakotuna, K. P. Esselle, L. Matekovits and M. Heimlich, "Reconfigurable half-width microstrip leaky-wave antenna for fixed-frequency beam scanning," *2013 7th European Conference on Antennas and Propagation (EuCAP)*, Gothenburg, 2013, pp. 1314-1317.

[7]   D. K. Karmokar, D. N. P. Thalakotuna, K. P. Esselle, M. Heimlich and L. Matekovits, "Fixed-frequency beam steering from a stub-loaded microstrip leaky-wave

antenna," *2013 International Symposium on Electromagnetic Theory*, Hiroshima, 2013, pp. 436-439.

[8]   M. Wang, H. F. Ma, H. C. Zhang, W. X. Tang, X. R. Zhang and T. J. Cui, "Frequency-Fixed Beam-Scanning Leaky-Wave Antenna Using Electronically Controllable Corrugated Microstrip Line," in *IEEE Transactions on Antennas and Propagation*, vol. 66, no. 9, pp. 4449-4457, Sept. 2018.

[9]   D. K. Karmokar and K. P. Esselle, "Fixed-frequency leaky-wave antenna for simultaneous forward and backward scanning," 2014 IEEE Antennas and Propagation Society International Symposium (APSURSI), Memphis, TN, 2014, pp. 1794-1795.

[10]   Potters Industries LLC, July 2016. [Online]. Available: http://www.pottersbeads.com/

[11]   J. M. Parrow et al., "On the Bandwidth of a Microparticle-Based Component Responsive to Magnetostatic Fields," in *IEEE Transactions on Electromagnetic Compatibility*, vol. 59, no. 4, pp. 1053-1059, Aug. 2017.

[12]   A. Iftikhar et al., "On using Magneto-static Responsive particles as switching elements to reconfigure microwave filters," *2016 IEEE International Conference on Electro Information Technology (EIT)*, Grand Forks, ND, 2016, pp. 0192-0195.

[13]   A. Iftikhar et al., "A printed dipole reconfigured with magneto-static responsive structures that do not require a directly connected biasing circuit," *2016 IEEE International Symposium on Antennas and Propagation (APSURSI)*, Fajardo, 2016, pp. 1057-1058.

[14]   A. Iftikhar, J. Parrow, S. Asif, J. Allen, M. Allen and B. D. Braaten, "Improving the efficiency of a reconfigurable microstrip patch using magneto-static field responsive structures," in *Electronics Letters*, vol. 52, no. 14, pp. 1194-1196, 7 7 2016.

[15] D. R. Jackson, C. Caloz and T. Itoh, "Leaky-Wave Antennas," in *Proceedings of the IEEE*, vol. 100, no. 7, pp. 2194-2206, July 2012.

[16] A. M. Patel and A. Grbic, "A Printed Leaky-Wave Antenna Based on a Sinusoidally-Modulated Reactance Surface," in *IEEE Transactions on Antennas and Propagation*, vol. 59, no. 6, pp. 2087-2096, June 2011.

[17] H. -Y. Yang, N. G. Alexopoulos and D. R. Jackson, "Microstrip open-end and gap discontinuities in a substrate-superstrate structure," in *IEEE Transactions on Microwave Theory and Techniques*, vol. 37, no. 10, pp. 1542-1546, Oct. 1989.

[18] M. Maeda, "An Analysis of Gap in Microstrip Transmission Lines," in *IEEE Transactions on Microwave Theory and Techniques*, vol. 20, no. 6, pp. 390-396, Jun. 1972.

[19] S. Eggermont, R. Platteborze and I. Huynen, "Investigation of metamaterial leaky wave antenna based on complementary split ring resonators," *2009 European Microwave Conference (EuMC)*, Rome, 2009, pp. 209-212.

[20] P. Benedek and P. Silvester, "Equivalent Capacitances for Microstrip Gaps and Steps," in *IEEE Transactions on Microwave Theory and Techniques*, vol. 20, no. 11, pp. 729-733, Nov. 1972.

[21] J. Cleveland, D. Mitra, J. Lewis, B. D. Braaten, J. Allen and M. Allen, "On the Placement of Particle Containing Cylindrical Cavities in a Grounded Dielectric Substrate to Change the Impedance of a Printed Reactive Surface", accepted for presentation at the 2019 IEEE International Symposium on Antennas and Propagation, Jul. 7 - 12, 2019, Atlanta GA, USA.

[22]   J. Cleveland, D. Mitra, J. Lewis, B. D. Braaten, J. Allen and M. Allen, "On Changing the

Impedance of a Reactive Surface Using Magneto-Static Responsive Particles", accepted

for presentation at the 2019 IEEE International Symposium on Antennas and

Propagation, Jul. 7 - 12, 2019, Atlanta GA, USA.